Arch. Min. Sci. **66** (2021), 2, 279-295

Electronic version (in color) of this paper is available: http://mining.archives.pl

DOI 10.24425/ams.2021.137462

ZHENMIN LUO[1,2*], LITAO LIU[1,2], SHUAISHUAI GAO[1,2], TAO WANG[1,2,3], BIN SU[1,2], LEI WANG[1,2], YONG YANG[1,2], XIUFANG LI[1]

SIMULATION STUDIES ON THE INFLUENCE OF OTHER COMBUSTIBLE GASES ON THE CHARACTERISTICS OF METHANE EXPLOSIONS AT CONSTANT VOLUME AND HIGH TEMPERATURE

Gas explosions are major disasters in coal mining, and they typically cause a large number of deaths, injuries and property losses. An appropriate understanding of the effects of combustible gases on the characteristics of methane explosions is essential to prevent and control methane explosions. FLACS software was used to simulate an explosion of a mixture of CH_4 and combustible gases (C_2H_4, C_2H_6, H_2, and CO) at various mixing concentrations and different temperatures (25, 60, 100, 140 and 180°C). After adding combustible gases to methane at a constant volume and atmospheric pressure, the adiabatic flame temperature linearly increases as the initial temperature increases. Under stoichiometric conditions (9.5% CH_4-air mixture), the addition of C_2H_4 and C_2H_6 has a greater effect on the adiabatic flame temperature of methane than H_2 and CO at different initial temperatures. Under the fuel-lean CH_4-air mixture (7% CH_4-air mixture) and fuel-rich mixture (11% CH_4-air mixture), the addition of H_2 and CO has a greater effect on the adiabatic flame temperature of methane. In contrast, the addition of combustible gases negatively affected the maximum explosion pressure of the CH_4-air mixture, exhibiting a linearly decreasing trend with increasing initial temperature. As the volume fraction of the mixed gas increases, the adiabatic flame temperature and maximum explosion pressure of the stoichiometric conditions increase. In contrast, under the fuel-rich mixture, the combustible gas slightly lowered the adiabatic flame temperature and the maximum explosion pressure. When the initial temperature was 140°C, the fuel consumption time was approximately 8-10 ms earlier than that at the initial temperature of 25°C. When the volume fraction of the combustible gas was 2.0%, the consumption time of fuel reduced by approximately 10 ms compared with that observed when the volume fraction of flammable gas was 0.4%.

Keywords: Constant volume, Volume fraction of combustible gas, Initial temperature, adiabatic flame temperature, Maximum explosion pressure

[1] XI'AN UNIVERSITY OF SCIENCE AND TECHNOLOGY, SCHOOL OF SAFETY SCIENCE & ENGINEERING, 58, YANTA MID. RD., XI'AN, 710054, SHAANXI, PR CHINA

[2] SHAANXI KEY LABORATORY OF PREVENTION AND CONTROL OF COAL FIRE, 58, YANTA MID. RD, XI'AN, 710054, SHAANXI, PR CHINA

[3] XI'AN UNIVERSITY OF SCIENCE AND TECHNOLOGY, POSTDOCTORAL PROGRAM, 58, YANTA MID. RD., XI'AN 710054, SHAANXI, PR CHINA

* Corresponding author: zmluo@xust.edu.cn

Nomenclature

t – time;
β_v – volume porosity, a dimensionless parameter;
ρ – density, $\mathrm{kgm^{-3}}$;
χ_j – the length coordinate in the j direction, m;
β_j – the area porosity in the j direction;
u_j – the mean velocity in the j direction, $\mathrm{ms^{-1}}$;
$\dot{m}$ – mass rate, $\mathrm{kgs^{-1}}$;
V – volume, $\mathrm{m^3}$;
u_i – mean velocity in the i direction, $\mathrm{ms^{-1}}$;
P – absolute pressure, Pa;
σ_{ij} – stress tensor, $\mathrm{Nm^{-2}}$
$F_{\omega,i}$ – flow resistance due to walls;
$F_{o,i}$ – flow resistance due to sub-grid obstructions in the i direction, pa;
ρ_0 – initial density, $\mathrm{kgm^{-3}}$;
g_i – gravitational acceleration in the i direction, $\mathrm{ms^{-2}}$;
h – specific enthalpy, $\mathrm{Jkg^{-1}}$;
μ_{eff} – effective viscosity, Pa·s;
σ_h – Prandtl-Schmidt number of enthalpy;
D_p – diffusion coefficient of particle;
D_t – diffusion coefficient of turbulence;
$\dot{Q}$ – heat rate, $\mathrm{Js^{-1}}$;
Υ_{fuel} – the fuel reaction rate;
σ_{fuel} – Prandtl-Schmidt number of fuel;
R_{fuel} – reaction rate for fuel, $\mathrm{kgm^{-3}s^{-1}}$;
k – turbulent kinetic energy, $\mathrm{m^2s^{-2}}$;
σ_k – Prandtl-Schmidt number of turbulent kinetic energy;
P_k – production of turbulent kinetic energy, $\mathrm{kg\,m^{-1}s^{-3}}$;
ε – the dissipation of turbulent kinetic energy, $\mathrm{m^2s^{-2}}$;
σ_ε – Prandtl-Schmidt number of dissipation of turbulent kinetic energy;
P_ε – production of dissipation of turbulent kinetic energy;
C_2 – constant in the k-ε equation, typically $C_2 = 1.92$.
$P_{\max}$ – maximum explosion pressure
T_f – adiabatic flame temperature
T_0 – initial temperature

1. Introduction

The depletion of fossil fuels and the urgent need to reduce the environmental pollution caused by combustion have promoted research on the combustion characteristics of alternative fuels. Methane is widely recognised as an important energy source to replace traditional fossil fuels because it has a number of advantages, such as wide distribution and rich reserves.

Methane is the main component of fuels such as natural gas and coal mine gas, and is widely used in civil and industrial applications. As a chemical raw material, it can be used to produce acetylene, hydrogen, and synthetic ammonia. Preventing accidental explosions due to their release into the atmosphere in the process of methane production is a key issue in the use, storage and transportation of fuel. Many scholars have conducted a large number of studies on the explosion characteristics of methane, and they revealed the explosion parameters under different conditions, such as the explosion limit [1-3], explosion pressure [4-9] and flame propagation [10-12]. In addition, the influence of other combustible gases on the explosion characteristics of methane has also been extensively studied [13-15].

The gas composition generated by spontaneous coal combustion in a high-temperature environment in a mine fire area is extremely complex. Due to the low-temperature oxidation or pyrolysis of coal, a variety of combustible and explosive gases are produced, such as CH_4, CO, H_2, C_2H_6, C_2H_4, C_3H_8, and C_2H_2 [16,17]. The explosive characteristics of flammable gas mixtures are determined under various conditions [18-20]. The effects of flammable gases on the explosion characteristics of CH_4 were investigated. C_2H_6, C_2H_4, CO, H_2 and their mixtures expand the flammable range of methane and increase the explosion risk of methane [3]. Compared with different combustible gases, hydrogen has a greater impact on methane explosion characteristics [21]. Experiments on the explosion limit of methane and hydrogen at different initial temperatures and pressures show that the flammable zone becomes wider as the initial temperature increases and becomes narrower as the initial pressure increases [22]. In recent years, numerous scholars have studied the explosion characteristics of methane under different conditions through numerical simulations [23-25]. However, numerical simulations of the effects of different gases on the maximum explosion pressure and temperature of methane have been studied less by using FLACS (a professional simulation software for explosions) at different initial temperatures in closed vessels [26].

Based on this practical problem, numerical simulations of methane explosions with different additions of flammable gases, such as C_2H_4, C_2H_6, H_2 and CO, at different initial temperatures (25, 60, 100, 140 and 180°C) were performed to investigate the effects of flammable gases on the maximum explosion pressure and temperature by using FLACS software. Data on the deflagration characteristics of fuel-air mixtures are required in various fields related to deflagration phenomena: design of pressure vessels; design of venting systems; and safety proposal for the use of fuels. This information is significant for understanding the variation in combustion properties under various conditions. Further studies on the effect of flammable gases on methane under various conditions will be summarised in our next study.

2. Physical modes and simulation settings

2.1. Physical model

After the flammable gas begins to explode, the flame rapidly propagates around the gas. A strong chemical reaction occurs at the unburned interface, promoting energy transformation and a change in the material. The most significant features are the high temperature and pressure and the intense burning flame. The internal explosion reaction in a spherical explosion tank serves as a physical model of the explosion of multiple gases in a confined space, as shown in Fig. 1.

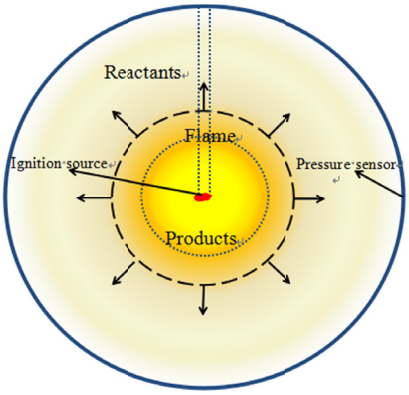

Fig. 1. Physical model of reaction inside an explosive tank

2.2. Mathematical model

1) Basic hypothesis

A gas explosion in a closed space is a complex chemical reaction and is accompanied by a flow process. When describing this reaction, we should assume the following: the internal gas is a real gas with all the associated properties. The explosion process of the gas is a simple step. The equipment is completely closed, and heat is not required. The process of exchange and explosion is adiabatic.

2) Basic equation

The flame propagation is described by a β-flame model, and the wall surface function is applied to the wall area near the wall. The β-flame model is applied with correlations of both the laminar and turbulent burning velocities that originate from the experiments. The conservation equations for the mass, momentum, enthalpy, and mass fraction of species, enclosed by the ideal gas law, are included. These equations are similarly expressed as follows.

Conservation of mass:

$$\frac{\partial}{\partial t}\left(\beta_v \rho\right)+\frac{\partial}{\partial \chi_j}\left(\beta_j \rho u_j\right)=\frac{\dot{m}}{v} \tag{1}$$

Momentum equation:

$$\frac{\partial}{\partial t}\left(\beta_v \rho u_j\right)+\frac{\partial}{\partial \chi_j}\left(\beta_j \rho u_j u_j\right)=$$

$$=-\beta_v \frac{\partial p}{\partial \chi_j}+\frac{\partial}{\partial \chi_j}\left(\beta_j \sigma_{ij}\right)+F_{o,i}+\beta_v F_{\omega,i}+\beta_v\left(\rho-\rho_0\right) g_i \tag{2}$$

$$F_{o,i}=-\rho\left|\frac{\partial \beta}{\partial \chi_j}\right| u_i \left|u_i\right| \tag{3}$$

Transport equation for enthalpy:

$$\frac{\partial}{\partial t}\left(\beta_v \rho h\right)+\frac{\partial}{\partial \chi_j}\left(\beta_j \rho u_j h\right)=\frac{\partial}{\partial \chi_j}\left(\beta_j \frac{\mu_{eff}}{\sigma_h}\frac{\partial h}{\partial \chi_j}\right)+\beta_v \frac{D_p}{D_t}+\frac{\dot{Q}}{V} \tag{4}$$

Transport equation for fuel mass fraction:

$$\frac{\partial}{\partial t}\left(\beta_v \rho \Upsilon_{fuel}\right)+\frac{\partial}{\partial \chi_j}\left(\beta_j \rho u_j \Upsilon_{fuel}\right)=\frac{\partial}{\partial \chi_j}\left(\beta_j \frac{\mu_{eff}}{\sigma_{fuel}}\frac{\partial \Upsilon_{fuel}}{\partial \chi_j}\right)+R_{fuel} \tag{5}$$

During the numerical simulation of the closed space, the flow field is described by the equation set *k*-*ε*, and the turbulence change is expressed. FLACS uses a Reynold-averaged Navier-Stokes (RANS) approach based on the standard *k*-*ε* model to close the equations. It is an eddy viscosity model that solves two additional transport equations, one for turbulent kinetic energy and one for dissipation of turbulent kinetic energy.

Transport equation for turbulent kinetic energy:

$$\frac{\partial}{\partial t}\left(\beta_v \rho k\right)+\frac{\partial}{\partial \chi_j}\left(\beta_j \rho u_j k\right)=\frac{\partial}{\partial \chi_j}\left(\beta_j \frac{\mu_{eff}}{\sigma_k}\frac{\partial k}{\partial \chi_j}\right)+\beta_v P_k-\beta_v \rho \varepsilon \tag{6}$$

Transport equation for the dissipation rate of turbulent kinetic energy:

$$\frac{\partial}{\partial t}\left(\beta_v \rho \varepsilon\right)+\frac{\partial}{\partial \chi_j}\left(\beta_j \rho u_j \varepsilon\right)=\frac{\partial}{\partial \chi_j}\left(\beta_j \frac{\mu_{eff}}{\sigma_\varepsilon}\frac{\partial \varepsilon}{\partial \chi_j}\right)+\beta_v P_\varepsilon-C_2 \beta_v \rho \frac{\varepsilon^2}{k} \tag{7}$$

More specific and detailed information regarding the FLACS code can be found in the FLACS manual [27].

2.3. Numerical Method

The author's mathematical model is based on FLACS software to simulate the convection diffusion of each component of other fires or explosions. The principle of FLACS software is to use the finite volume method to solve the compressible N-S equation using a three-dimensional Cartesian grid.

2.4. Geometric model and grid partition

This paper reports the simulation results with a spherical explosion vessel (a diameter of 336.8 mm). The sensor is mounted on the inner wall, and the ignition point is at the center of the container. In this simulation, the boundary conditions are $u = w = v = 0$ on the wall and along the wall of the container, and the velocity is steady. For the normal vector, the temperature, density gradient and pressure are 0. In this simulation, a uniform grid is used in the entire calculation area. As the calculation is performed using a real grid, the calculation area is a step boundary near the real boundary. In the computing area, the grid independence was verified by using 20 grids, 27 grids, and 34 grids in three directions of X, Y, and Z, and the calculated area

is composed of 8,000 grids, 19,683 grids, and 39,304 grids. More intensive grids cannot increase the accuracy and lengthen the solution time. Therefore, 27 grids are divided in three directions of X, Y, and Z.

2.5. Simulation conditions

The simulated gases are CH_4, CO, C_2H_6, C_2H_4 and H_2. The starting temperatures are 25, 60, 100, 140 and 180°C. The ambient humidity and the initial pressure are the same as those in the experimental conditions. The volume fraction of added fuel (C_2H_6, C_2H_4, CO, and H_2) in CH_4 was 0.4-2.0% with an interval of 0.4. The volume fractions of CH_4 in the experiments were 7, 9.5, and 11%. The flow state of combustible gas is a macroscopic static state.

3. Reliability verification of numerical model

Many validation studies have contributed to the wide acceptance of the FLACS code as a reliable tool for the prediction of fuel-air explosions occurring in real processing areas. To verify the capability of the FLACS code to predict methane-air explosions under different conditions, validations applied at different temperatures and concentrations are described in this section.

3.1. Experimental settings and conditions

The experimental apparatus was similar to that used in the previous work as shown in Fig. 2. Experiments were performed in a 20-L spherical explosive vessel with a quartz glass window 110 mm in diameter using an electric spark (1 J) as the ignition source. All experiments were conducted at high temperature and ambient pressure (0.1 MPa), with relative humidity ranging from 52 to 73%. The initial gas temperature of this spherical tank was set to 25, 60 and 100°C.

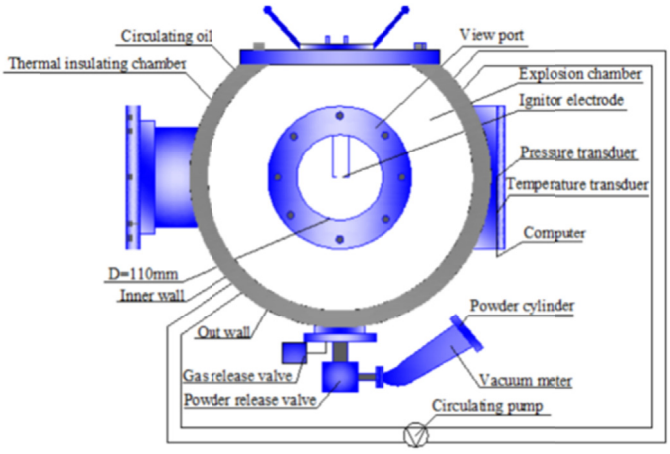

Fig. 2. Schematic of experimental setup

3.2. Experiment validation

For methane -air mixture explosions, the results of the maximum explosion pressure obtained from the simulation are very close to the results of other authors [26]. The experimental results [28] and simulation results of the maximum explosion pressure of the methane-carbon monoxide-air mixture in a 20-L spherical vessel under high temperature and atmospheric pressure are shown in Fig. 3. The variation trends of the simulated value and experimental value are similar. There are some deviations between the two sets of results, and the standard deviation ranges from 0.03 to 0.14. In the simulation process, the model is in an adiabatic closed state, and there is no loss of heat. The cooling of the tank and the leakage of the gas leads to heat loss, explaining the differences between the experimental results and the simulation. Therefore, the numerical method used in this paper is of high credibility and can be useful for research.

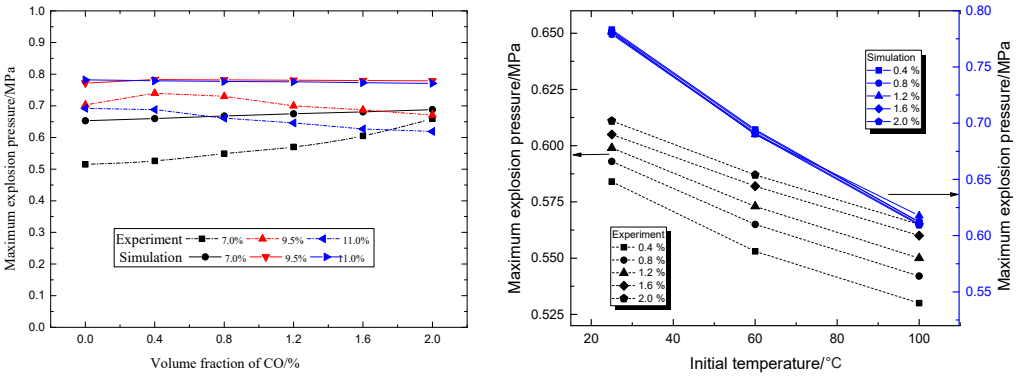

(a) the effects of the volume fraction of CO on the maximum explosion pressure at 25°C

(b) the effects of the initial temperature on the maximum explosion pressure of CH_4-CO-air mixture

Fig. 3. Experiment and numerical results of the maximum explosion pressure of the CH_4-CO-air mixture at different initial temperatures

4. Results

4.1. Effect of combustible gas on methane explosion characteristics at different initial temperatures

We tentatively propose that T_f of the gas mixture increases and P_{max} of the gas mixture decreases as the initial temperature increases. The data are fitted by Eq. (8) and Eq. (9):

$$T_f = a + bT_0 \tag{8}$$

$$P_{max} = c + dT_0 \tag{9}$$

The slopes and intercepts of the correlations P_{max} and T_f for 7% methane-air mixtures are given in Table 1. The effects of the initial temperature on the adiabatic flame temperature and maximum explosion pressure of 7% CH_4 are shown in Fig. 4. When four kinds of combustible

gases (C_2H_6, C_2H_4, H_2, and CO) are added to 7% CH_4, the adiabatic flame temperature of the mixed gas linearly increases with increasing temperature. When 0.4% combustible gas is added, with increasing initial temperature, the adiabatic flame temperature increases by 3.4%, 3.2%, 3%, and 3.3%, respectively. The addition of C_2H_4 has the greatest effect on the adiabatic flame temperature of methane. When 1.2% combustible gas is added, the adiabatic flame temperature of methane increases by 4.7%, 4.3%, 3.1%, and 3.2%, respectively. When 2.0% combustible gas is added, the adiabatic flame temperature of methane increases by 5.6%, 5.0%, 3.3%, and

TABLE 1

The slopes and intercepts of the correlations of 7% methane between P_{max}, T_f and temperature

Gas	a			b			c			d		
	0.4	**1.2**	**2.0**	**0.4**	**1.2**	**2.0**	**0.4**	**1.2**	**2.0**	**0.4**	**1.2**	**2.0**
C_2H_6	2446.9	2339.2	2209.5	0.529	0.713	0.796	0.818	0.816	0.800	–0.002	–0.002	–0.002
C_2H_4	2459.8	2396.1	2309.6	0.507	0.673	0.744	0.815	0.827	0.818	–0.002	–0.002	–0.002
CO	2446.5	2452.5	2457.1	0.534	0.518	0.526	0.813	0.811	0.809	–0.002	–0.002	–0.002
H_2	2451.5	2459.1	2457.6	0.468	0.507	0.511	0.806	0.815	0.815	–0.002	–0.002	–0.002

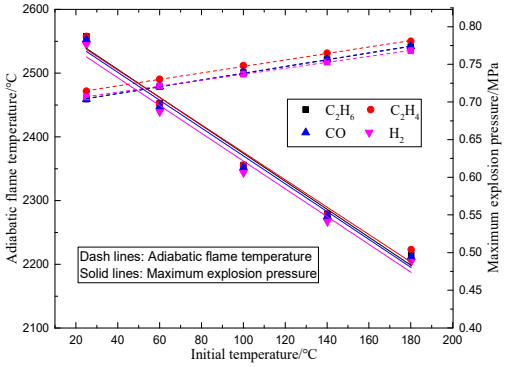

(a) 0.4%

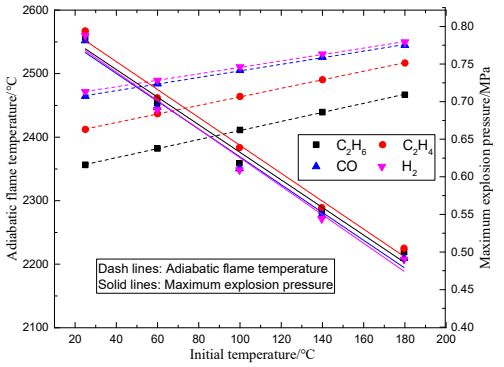

(b) 1.2%

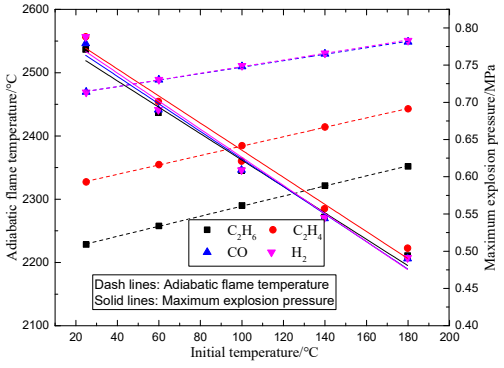

(c) 2.0%

Fig. 4. Effect of initial temperature on the explosion characteristics of 7% methane and combustible gas

3.2%, respectively. After adding 1.2% and 2.0% combustible gas, the addition of CO and H_2 has the greatest effect on the adiabatic flame temperature of methane, compared with C_2H_6 and C_2H_4. However, with increasing initial temperature, the maximum explosion pressure of methane showed a linearly decreasing trend, and the decrease was maintained within 36% to 37%. Adding four kinds of combustible gases with different concentrations, the maximum explosion pressure of methane showed an increasing trend.

The effects of the initial temperature on the adiabatic flame temperature and maximum explosion pressure of 9.5% CH_4 are shown in Fig. 5. After adding four kinds of gas combustibles, the adiabatic flame temperature of methane linearly increased with increasing temperature. The slopes and intercepts of the correlations P_{max} and T_f for 9.5% methane-air mixtures are given in Table 2. When 0.4% of the other four combustible gases were added, with increasing the initial temperature, the adiabatic flame temperature of methane increased by 4.9%, 4.9%, 5.6%, and 5.6%, respectively. When 1.2% of the other four combustible gases were added, the adiabatic flame temperature of methane increased by 3.2%, 3.3%, 5%, and 5%. When 2.0% of the other four combustible gases were added, the adiabatic flame temperature of methane increased by

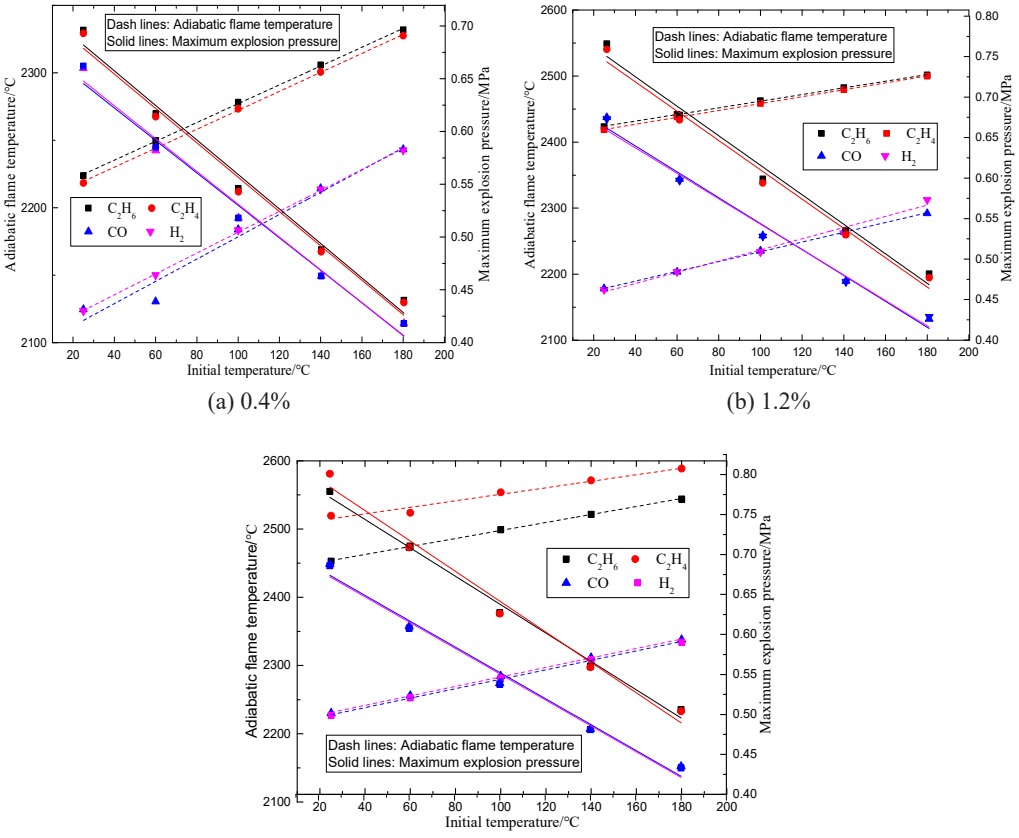

(a) 0.4%

(b) 1.2%

(c) 2.0%

Fig. 5. Effect of initial temperature on the explosion characteristics of 9.5% methane and combustible gas

2.7%, 2.8%, 4.8%, and 4.8%, respectively. After adding four kinds of combustible gases, the percentage increase of H_2 and CO to the adiabatic flame temperature of methane was larger than that of C_2H_4 and C_2H_6. Contrary to the change rule of the maximum explosion temperature, with the increase of the initial temperature, the maximum explosion pressure of methane showed a decreasing trend, and the change range was not significantly affected by the types and volume fractions of the other four gases, with a decrease of approximately 37 %. At the same temperature, the addition of C_2H_4 and C_2H_6 had a greater effect on the maximum explosion pressure of methane than that of H_2 and CO.

TABLE 2

The slopes and intercepts of the correlations of 9.5% methane between P_{max}, T_f and temperature

Gas	a			b			c			d		
	0.4	**1.2**	**2.0**	**0.4**	**1.2**	**2.0**	**0.4**	**1.2**	**2.0**	**0.4**	**1.2**	**2.0**
C_2H_6	2207.4	2411.6	2439.3	0.698	0.504	0.586	0.723	0.796	0.832	–0.002	–0.002	–0.002
C_2H_4	2202.0	2406.2	2502.2	0.703	0.522	0.477	0.720	0.789	0.815	–0.002	–0.002	–0.002
CO	2096.0	2160.0	2210.7	0.826	0.739	0.692	0.684	0.702	0.715	–0.002	–0.002	–0.002
H_2	2104.5	2152.0	2213.9	0.774	0.847	0.477	0.687	0.698	0.713	–0.002	–0.002	–0.002

The effects of the initial temperature on the adiabatic flame temperature and maximum explosion pressure of 11% CH_4 are shown in Fig. 6. When the volume fraction of methane was 11%, as the initial temperature increased, the adiabatic flame temperature of methane linearly rose. The slopes and intercepts of the correlations P_{max} and T_f for 11% methane-air mixtures are given in Table 3. When 0.4% combustible gases were added, with increasing initial temperature, the adiabatic flame temperature of methane increased by 4.9%, 4.7%, 4.4%, and 4.4%, respectively. When 1.2% combustible gases were added, the adiabatic flame temperature of methane increased by 5.8%, 5.4%, 4.6%, and 4.6%, respectively. When 2.0% of the four kinds of combustible gases were added, the adiabatic flame temperature of methane increased by 9.8%, 5.8%, 4.7%, and 4.8%, respectively. After adding four kinds of combustible gases, the percentage increase of H_2 and CO to the adiabatic flame temperature of methane is larger than that of C_2H_4 and C_2H_6. At this time, the maximum explosion pressure showed a downward trend with increasing initial temperature.

TABLE 3

The slopes and intercepts of the correlations of 11% methane between P_{max}, T_f and temperature

Gas	a			b			c			d		
	0.4	**1.2**	**2.0**	**0.4**	**1.2**	**2.0**	**0.4**	**1.2**	**2.0**	**0.4**	**1.2**	**2.0**
C_2H_6	2314.0	2180.8	2014.3	0.730	0.819	1.195	0.807	0.791	0.760	–0.002	–0.002	–0.002
C_2H_4	2331.4	2241.7	2147.4	0.758	0.786	0.811	0.811	0.802	0.792	–0.002	–0.002	–0.002
CO	2366.8	2348.2	2329.2	0.686	0.704	0.724	0.809	0.806	0.801	–0.002	–0.002	–0.002
H_2	2366.8	2356.7	2327.4	0.682	0.707	0.717	0.809	0.805	0.799	–0.002	–0.002	–0.002

In all cases, when the initial pressure and the volume of a flammable mixture within the explosion vessel remained unchanged, one of the causes of this phenomenon was the decrease in density for the burning charge, which releases a lower heat amount, thereby delivering a decrease in the explosion pressure. For the 7% CH_4-air mixture, this phenomenon is attributed to

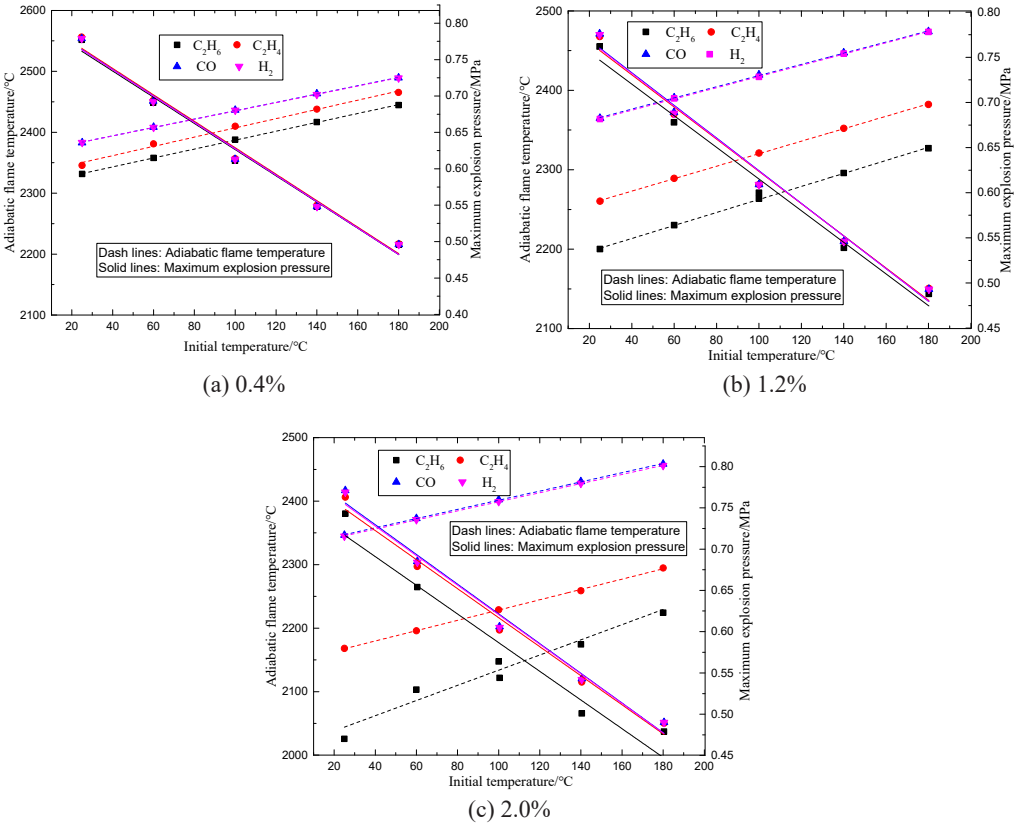

(a) 0.4%

(b) 1.2%

(c) 2.0%

Fig. 6. Effect of initial temperature on explosion characteristics of 11% methane and combustible gas

the enrichment of the fuel-air ratio by the mixed gas. The oxygen consumed in the reaction of flammable gas and oxygen is lower than that in the reaction of methane and oxygen under the same conditions. The reaction can be performed more completely, which leads to increases in maximum explosion pressure. For the 9.5% CH_4-air mixture, this volume can be completely consumed in air, which should result in the most violent explosion. In addition, for the 11% CH_4-air mixture, the presence of flammable gas also exacerbated the degree of oxygen depletion and led to slight decreases in the maximum explosion pressure.

4.2. Effect of combustible gas on the methane explosion process under different initial temperatures

At 0 ms, 20 ms, 26 ms, 40 ms, and 47 ms, the product concentration (PROD) and the velocity vector and scalar (VVEC and UVW) of the flame front during the 9.5% methane explosion at 25°C and 140°C are shown in Fig. 7 and Fig. 8. Fig. 7 shows the change in the product concentration of 9.5% CH_4 during the explosion at 25°C and 140°C. When the initial temperature was 25°C, the explosive product did not completely fill the container at 47 ms, and the reaction

was still proceeding. When the initial temperature was 140°C, the reactor was filled with explosion products at approximately 40 ms, the reaction was complete, and the pressure reached its maximum. In addition, few differences were observed in terms of the distributions of the concentration for explosion products. Fig. 8 shows the effects of the initial temperature on the velocity field of 9.5% methane during the explosion at 25°C and 140°C. When the initial temperature

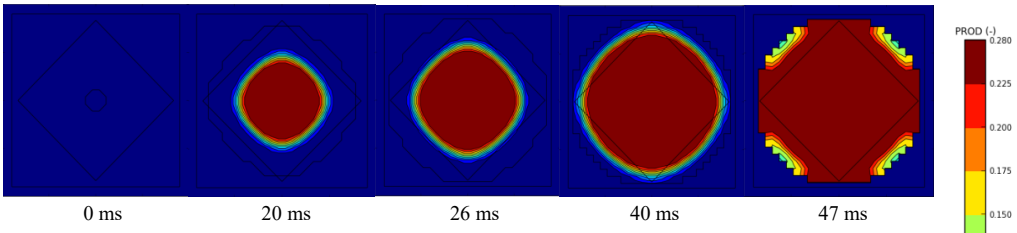

(a) The change in the product concentration of 9.5% CH_4 during explosion at 25°C

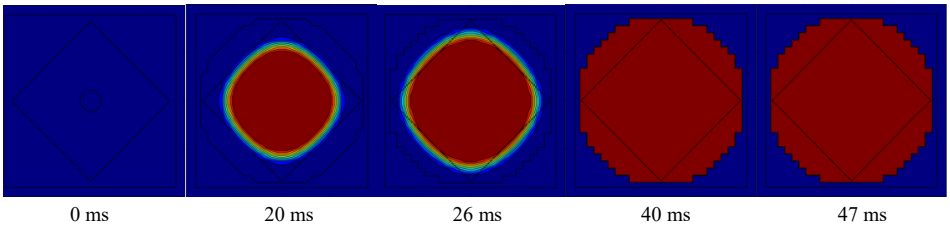

(b) The change in the product concentration of 9.5% CH_4 during explosion at 140°C

Fig. 7. Effects of initial temperature on the flame front of methane explosion

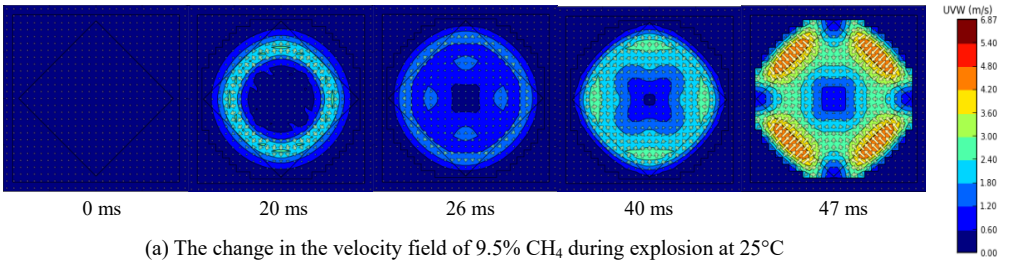

(a) The change in the velocity field of 9.5% CH_4 during explosion at 25°C

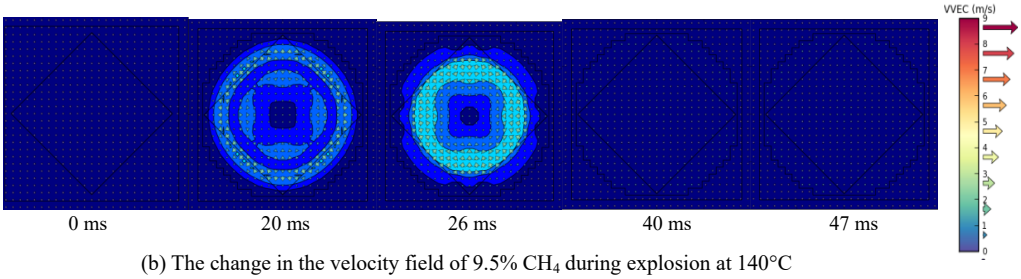

(b) The change in the velocity field of 9.5% CH_4 during explosion at 140°C

Fig. 8. Effects of initial temperature on velocity field of methane explosion

was 25°C, the flame propagated from the initiation point of the model within 0~20 ms. In the range of 20~26 ms, the flame front touched the wall of the vessel and propagated backwards. At 47 ms, the propagation velocity is approximately 6 m/s. According to the distribution of the gas velocity, the propagation velocity at the initial temperature of 140°C was far greater than that at 25°C. Before 20 ms, the explosive flame front had reached the wall and propagated in the opposite direction. The explosive reaction had finished within 26~40 ms, and the products were completely distributed in the explosion vessel. When the initial temperature was 140°C,

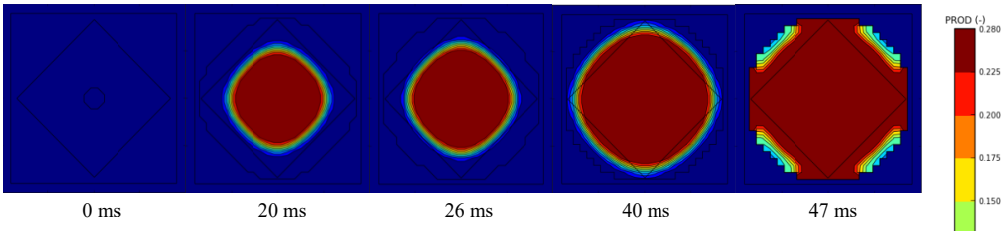

(a) The change in the product concentration during the explosion of 0.4% C_2H_6 and 9.5% CH_4

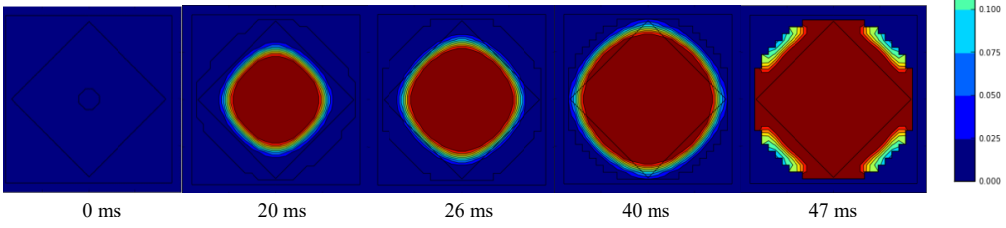

(b) The change in the product concentration during the explosion of 0.4% H_2 and 9.5% CH_4

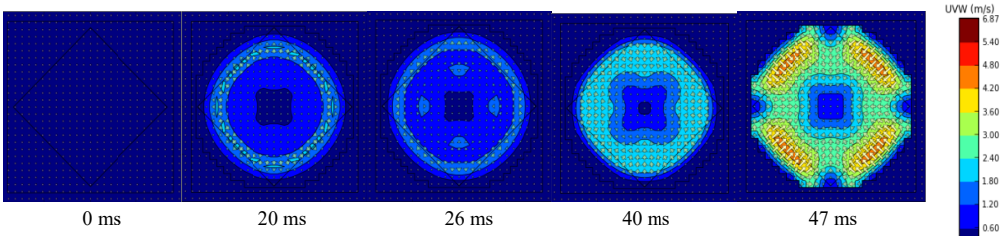

(c) The change in the velocity field during the explosion of 0.4% C_2H_6 and 9.5% CH_4

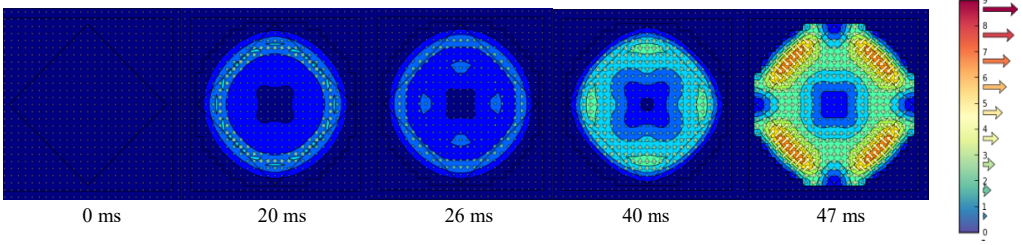

(d) The change in the velocity field during the explosion of 0.4% H_2 and 9.5% CH_4

Fig. 9. Effects of 0.4% H_2 and C_2H_4 on the product concentration and the velocity vector and scalar of the methane explosion

the fuel consumption time was approximately 8~10 ms earlier than that at the initial temperature of 25℃. In summary, the increasing initial temperature accelerated the propagation velocity of methane.

At 0 ms, 20 ms, 26 ms, 40 ms, and 47 ms, when 2% C_2H_6 and H_2 were added, the product concentration (PROD) and the velocity vector and scalar (VVEC and UVW) of the flame front during the 9.5% methane explosion at 25°C are shown in Fig. 9 and Fig. 10. The addition of 0.4% H_2 and C_2H_6 gas to the methane explosion product concentration and velocity field results in changes noted in Fig. 9. As shown in Fig. 9 (a) and (c), when 0.4% C_2H_6 was added, the flame

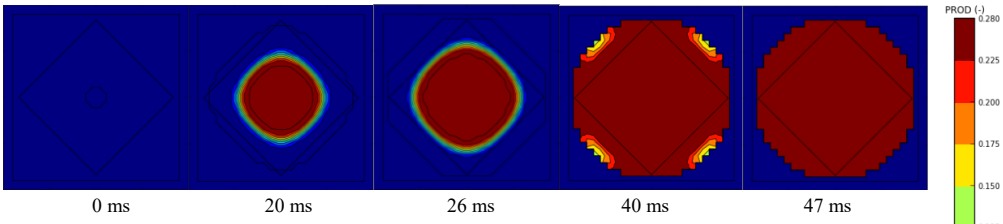

(a) The change in the flame front during the explosion of 2% C_2H_6 and 9.5% CH_4

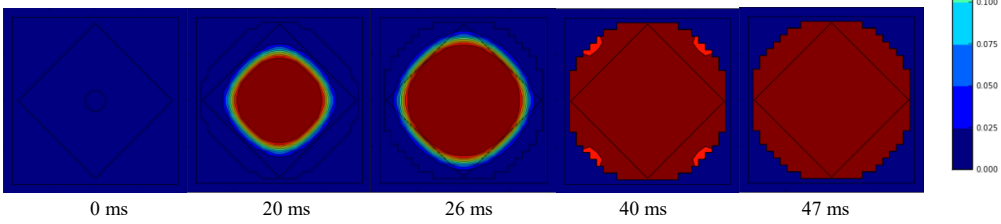

(b) The change in the flame front during the explosion of 2% H_2 and 9.5% CH_4

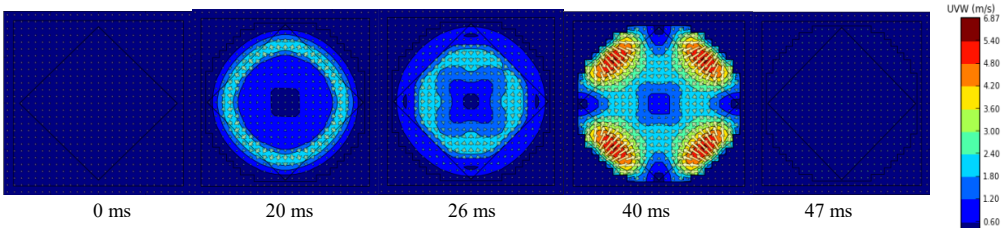

(c) The change in the velocity field during the explosion of 2% C_2H_6 and 9.5% CH_4

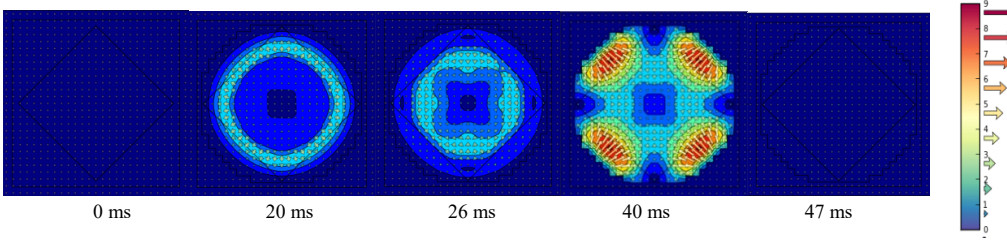

(d) The change in the velocity field during the explosion of 2% H_2 and 9.5% CH_4

Fig. 10. Effects of 2.0% H_2 and C_2H_4 on the product concentration and the velocity vector and scalar of the methane explosion

front extended to the periphery in the form of an approximately spherical surface. It was filled with explosive containers between 40 and 47 ms. It can be seen from the velocity field that after the explosion reaction, the propagation velocity quickly accelerates to 5.5 m/s at 47 ms. From the perspective of the explosion process, the effect of adding 0.4% H_2 to methane is not much different from that of adding 0.4% C_2H_6. Similar results can be seen between 40 and 47 ms. When the fuel was exhausted, the direction of the explosion began to reverse. The propagation velocity was approximately 5.5 m/s at 47 ms.

Fig. 10 shows the changes in the product concentration and velocity field during the methane explosion, when 2% of C_2H_6 and H_2 were added. As noted in Fig. 10 (a) and (c), when 2% C_2H_6 was added, the flame front also extended to the surroundings in the form of an approximate sphere. It was filled with an explosive container at a time between 26 and 40 ms. At 20 ms, the direction of the explosion propagation changed from forward to reverse propagation to ultimately achieving the maximum speed (approximately 7 m/s). The impact of 2.0% H_2 on the propagation velocity of methane explosions was similar to that of 2% C_2H_6 from 20 to 40 ms.

In summary, the effects of combustible gas with different volume fractions at a normal temperature on methane explosion were compared. When the volume fraction of combustible gas was 2%, the time of fuel consumption was approximately 10 ms reduced compared with that of combustible gas when the volume fraction of combustible gas was 0.4%. In contrast, different gases had different effects on methane explosions. After the addition of C_2H_6 and H_2, the burnout time of the fuel in the explosion process was almost the same.

4. Conclusion

1) Under constant volume and normal pressure, when combustible gases (C_2H_6, C_2H_4, CO, H_2) were added to a 7% methane-air mixture, the adiabatic flame temperature linearly increased as the initial temperature increased. The addition of CO and H_2 had a greater effect on the extent of the increase in the adiabatic flame temperature. Otherwise, the maximum explosion pressure linearly declined with increasing initial temperature, and the extent of the decrease was almost the same. The impact of the combustible gas volume fraction on the variation trend of the adiabatic flame temperature and maximum explosion pressure was inapparent within the simulation range.
2) For the 9.5% methane-air mixture, the adiabatic flame temperature linearly increased along with the initial temperature after adding the four combustible gases. C_2H_6 and C_2H_4 had a considerable influence on the increased range of the adiabatic flame temperature. In addition, as the initial temperature increased, the maximum explosion pressures all showed a linear downward trend. However, the maximum explosion pressures of C_2H_6 and C_2H_4 were greater than those of CO and H_2. Furthermore, the adiabatic flame temperature and maximum explosion pressure increased with increasing combustible gas volume fraction.
3) For the 11% methane-air mixture, the adiabatic flame temperature linearly increased with increasing initial temperature after adding four kinds of combustible gasses. CO and H_2 had a considerable influence on the increased range of the adiabatic flame temperature. The maximum explosion pressure linearly decreased as the initial temperature increased. Meanwhile, the adiabatic flame temperature and maximum explosion pressure declined as the volume fraction of combustible gas increased.

4) When the initial temperature was 140°C, the fuel consumption time was approximately 8-10 ms earlier than that at the initial temperature of 25°C. When the volume fraction of the combustible gas was 2.0%, the consumption time of fuel was reduced by approximately 10 ms compared with that observed when the volume fraction of flammable gas was 0.4%.

Acknowledgements

This work is funded by the National Natural Science Foundation of China (No. 51674193), the National Key Research and Development Program of China (No.2017YFC0804702), the Joint Fund Project of Shaanxi Province, China (No. 2019JLM-9) and China Postdoctoral Science Foundation (No. 2019-M-663780).

References

[1] Z. Li, M. Gong, E. Sun, J. Wu, Y. Zhou, *Effect of low temperature on the flammability limits of methane/nitrogen mixtures*. Energy **36**, 5521-5524 (2011). DOI: https://doi.org/10.1016/j.energy.2011.07.023

[2] B. Su, Z. Luo, T. Wang, J. Zhang, F. Cheng, *Experimental and principal component analysis studies on minimum oxygen concentration of methane explosion*. Int. J. Hydrog. Energy **45**, 12225-12235 (2020). DOI: https://doi.org/10.1016/j.ijhydene.2020.02.133

[3] T. Wang, Z. Luo, H. Wen, F. Cheng, J. Deng, J. Zhao, Z. Guo, J. Lin, K. Kang, W. Wang, *Effects of flammable gases on the explosion characteristics of CH4 in air*. J. Loss Prev. Process Ind. **49**, 183-190 (2017). DOI: https://doi.org/10.1016/j.jlp.2017.06.018

[4] G. Cui, S. Wang, J. Liu, Z. Bi, Z. Li, *Explosion characteristics of a methane / air mixture at low initial temperatures*. Fuel **234**, 886-893 (2018). DOI: https://doi.org/10.1016/j.fuel.2018.07.139

[5] M. Gieras, R. Klemens, G. Rarata, P. Wolan, *Determination of explosion parameters of methane-air mixtures in the chamber of 40 dm 3 at normal and elevated temperature*. J. Loss Prev. Process Ind. **19**, 263-270 (2006). DOI: https://doi.org/10.1016/j.jlp.2005.05.004

[6] H. Li, J. Deng, C.M. Shu, C.H. Kuo, Y. Yu, X. Hu, *Flame behaviours and deflagration severities of aluminium powder-air mixture in a 20-L sphere: Computational fluid dynamics modelling and experimental validation*. Fuel **276**, 118028 (2020). DOI: https://doi.org/10.1016/j.fuel.2020.118028

[7] M. Mitu, V. Giurcan, D. Razus, M. Prodan, D. Oancea, *Propagation indices of methane-air explosions in closed vessels*. J. Loss Prev. Process Ind. **47**, 110-119 (2017). DOI: https://doi.org/10.1016/j.jlp.2017.03.001

[8] M. Mitu, M. Prodan, V. Giurcan, D. Razus, D. Oancea, *Influence of inert gas addition on propagation indices of methane-air deflagrations*. Process Saf. Environ. Protect. **102**, 513-522 (2016). DOI: https://doi.org/10.1016/j.psep.2016.05.007

[9] B. Su, Z. Luo, T. Wang, C. Xie, F. Cheng, *Chemical kinetic behaviors at the chain initiation stage of CH4/H2/air mixture*. J. Hazard. Mater. **404**, 123680 (2021). DOI: https://doi.org/10.1016/j.jhazmat.2020.123680

[10] X.J. Gu, M.Z. Haq, M. Lawes, R. Woolley, *Laminar burning velocity and Markstein lengths of methane-air mixtures*. Combust. Flame. **121**, 41-58 (2000). DOI: https://doi.org/10.1016/S0010-2180(99)00142-X

[11] L. Liu, Z. Luo, T. Wang, F. Cheng, S. Gao, H. Liang, *Effects of initial temperature on the deflagration characteristics and flame propagation behaviors of CH4 and its blends with C2H6, C2H4, CO, and H2*. Energy Fuels **35**, 785-795 (2021). DOI: https://doi.org/10.1021/acs.energyfuels.0c03506

[12] Z. Luo, L. Liu, F. Cheng, T. Wang, B. Su, J. Zhang, S. Gao, C. Wang, *Effects of a carbon monoxide-dominant gas mixture on the explosion and flame propagation behaviors of methane in air*. J. Loss Prev. Process Ind. **58**, 8-16 (2019). DOI: https://doi.org/10.1016/j.jlp.2019.01.004

[13] M. Reyes, F. V Tinaut, A. Horrillo, A. Lafuente, *Experimental characterization of burning velocities of premixed methane-air and hydrogen-air mixtures in a constant volume combustion bomb at moderate pressure and temperature*. Appl. Therm. Eng. **130**, 684-697 (2018). DOI: https://doi.org/10.1016/j.applthermaleng.2017.10.165

[14] T. Wang, Z. Luo, H. Wen, J. Zhao, F. Cheng, C. Liu, Y. Xiao, J. Deng, *Flammability limits behavior of methane with the addition of gaseous fuel at various relative humidities*. Process Saf. Environ. Protect. **140**, 34 (2019). DOI: https://doi.org/10.1016/j.psep.2020.05.005

[15] T. Wang, Z. Luo, H. Wen, F. Cheng, L. Liu, *The explosion enhancement of methane-air mixtures by ethylene in a confined chamber*. Energy **214**, 119042 (2021). DOI: https://doi.org/10.1016/j.energy.2020.119042

[16] Y. Zhang, C. Yang, Y. Li, Y. Huang, J. Zhang, Y. Zhang, Q. Li, *Ultrasonic extraction and oxidation characteristics of functional groups during coal spontaneous combustion*. Fuel **242**, 287-294 (2019). DOI: https://doi.org/10.1016/j.fuel.2019.01.043

[17] J. Zhao, J. Deng, T. Wang, J. Song, Y. Zhang, C.M. Shu, Q. Zeng, *Assessing the effectiveness of a high-temperature-programmed experimental system for simulating the spontaneous combustion properties of bituminous coal through thermokinetic analysis of four oxidation stages*. Energy **169**, 587-596 (2019). DOI: https://doi.org/10.1016/j.energy.2018.12.100

[18] A.A. Pekalski, H.P. Schildberg, P.S.D. Smallegange, S.M. Lemkowitz, J.F. Zevenbergen, M. Braithwaite, H.J. Pasman, *Determination of the explosion behaviour of methane and propene in air or oxygen at standard and elevated conditions*. Process Saf. Environ. Protect. **83**, 421-429 (2005).

[19] K. Holtappels, *Report on the experimentally determined explosion limits, explosion pressures and rates of explosion pressure rise – Part 1: methane, hydrogen and propylene Contact*. Explosion **1**, 1-149 (2002).

[20] M. Gieras, R. Klemens, G., *Experimental Studies of Explosions of Methane-Air Mixtures in a Constant Volume Chamber*. Combust. Sci. Technol. 37-41 (2009). DOI: https://doi.org/10.1080/00102200802665102

[21] E. Salzano, F. Cammarota, A. Di Benedetto, V. Di Sarli, *Explosion behavior of hydrogen e methane / air mixtures.* J. Loss Prev. Process Ind. **25**, 443-447 (2012). DOI: https://doi.org/10.1016/j.jlp.2011.11.010

[22] K.L. Cashdollar, I.A. Zlochower, G.M. Green, R.A. Thomas, M. Hertzberg, *Flammability of methane, propane, and hydrogen gases*. J. Loss Prev. Process Ind. **13**, 327-340 (2000).

[23] H. Li, J. Deng, X. Chen, C.M. Shu, C.H. Kuo, X. Zhai, Q. Wang, X. Hu, *Transient temperature evolution of pulverized coal cloud deflagration in a methane-oxygen atmosphere*. Powder Technol. **366**, 294-304 (2020). DOI: https://doi.org/10.1016/j.powtec.2020.02.042

[24] S. Zhang, H. Ma, X. Huang, S. Peng, *Numerical simulation on methane-hydrogen explosion in gas compartment in utility tunnel*. Process Saf. Environ. Protect. **140**, 100-110 (2020). DOI: https://doi.org/10.1016/j.psep.2020.04.025

[25] Y. Zhu, D. Wang, Z. Shao, X. Zhu, C. Xu, Y. Zhang, *Investigation on the overpressure of methane-air mixture gas explosions in straight large-scale tunnels*. Process Saf. Environ. Protect. **135**, 101-112 (2019). DOI: https://doi.org/10.1016/j.psep.2019.12.022

[26] J. Deng, F. Cheng, Y. Song, Z. Luo, Y. Zhang, *Experimental and simulation studies on the influence of carbon monoxide on explosion characteristics of methane*. J. Loss Prev. Process Ind. **36**, 45-53 (2015). DOI: https://doi.org/10.1016/j.jlp.2015.05.002

[27] Gexcon, FLACS Manual. Gexcon, 2009.

[28] Z. Luo, R. Li, T. Wang, F. Cheng, Y. Liu, Z. Yu, S. Fan, X. Zhu, *Explosion pressure and flame characteristics of CO/CH4/air mixtures at elevated initial temperatures*. Fuel **268**, 117377 (2020). DOI: https://doi.org/10.1016/j.fuel.2020.117377